Journal of Materials Chemistry C

PAPER

The mechanical bending effect and mechanism of high performance and low-voltage flexible organic thin-film transistors with a cross-linked PVP dielectric layer†

Cite this: DOI: 10.1039/c3tc32460e

Mingdong Yi,[a] Yuxiu Guo,[ac] Jialin Guo,[a] Tao Yang,[a] Yuhua Chai,[c] Quli Fan,[a] Linghai Xie*[a] and Wei Huang*[ab]

Received 13th December 2013
Accepted 18th January 2014

DOI: 10.1039/c3tc32460e

www.rsc.org/MaterialsC

Low operational voltage flexible organic thin-film transistors (OTFTs) have been achieved using two layers of cross-linked PVP as the dielectric layer on a flexible polyimide (PI) substrate. At low operating voltages of −4 V, the flexible OTFTs showed good performances with high field-effect mobility (~0.56 $cm^2 V^{-1} s^{-1}$), low threshold voltage (~−0.82 V), high on/off current ratio (~10^5) and excellent electrical stability (~2 months). During a severe mechanical bending test (10^4 bending cycles and a bending radius of 0.75 mm) under ambient conditions, the flexible OTFTs still showed excellent electrical performance at the low operational voltage. Moreover, the effects of the mechanical bending on the electrical parameters of the flexible OTFTs were also systematically investigated. We found that the variations of the electrical parameters of the flexible OTFTs during the mechanical bending process were closely related to the distance effect of the spacing between stretched pentacene molecules and the doping effect of H_2O and O_2 which were induced by the mechanical bending strains. In comparison with previously reported flexible OTFTs, the research results showed that the distance effect and doping effect were mutually independent as well as mutually related during the mechanical bending process of the flexible OTFTs.

Introduction

Recently, flexible electronics have attracted extensive attention due to the advantages of mechanical flexibility, being lightweight and low fabrication costs and are being developed as next-generation electronics.[1–3] In the field of flexible electronics, flexible organic thin-film transistors (OTFTs) are considered as promising candidates for flexible displays, electronic skin, smart cards, *etc.*[4–6] Although the research on flexible OTFTs is just beginning, flexible OTFTs show excellent mechanical and electrical characteristics, and even some of the electrical parameters of flexible OTFTs are superior to those of rigid inorganic and organic TFTs.[7] However, despite recent progress to improve the mechanical and electrical characteristics of flexible OTFTs, most flexible OTFTs can only operate at a high operational voltage which restricts the range of their practical application.[8–10] In order to reduce the operational voltage of flexible OTFTs, the reported flexible OTFTs, which operate at low voltages (≤−5 V), usually use high-κ metal oxides and hybrid dielectrics composed of self-assembled monolayers (SAMs) on high-κ metal oxides as the dielectric layer.[11–13] However, the fabrication process of high-κ metal oxides requires expensive and complicated techniques which are incompatible with flexible plastic substrates. As one of the insulating polymer materials, cross-linked poly(4-vinylphenol) (PVP) has been extensively studied as the gate dielectric layer in rigid OTFTs. In addition to the general advantages of insulating polymer materials such as low temperature processing and excellent mechanical flexibility, cross-linked PVP film has the remarkable characteristic of a high dielectric constant, so it is very suitable to achieve low operational voltage flexible OTFTs.[14] However, during the cross-linking process of the cross-linked PVP film, many pinholes are usually generated which reduce its electrical insulation capacity, thus it is very easily broken-down under an electric field. To eliminate these pinholes and enhance the insulating capacity of the cross-linked PVP film, different cross-linking methods and agents are used, however these efforts also increase the complexity of the fabrication technology. Therefore, it is very significant to

[a]Center for Molecular Systems and Organic Devices (CMSOD), Key Laboratory for Organic Electronics & Information Displays (KLOEID) and Institute of Advanced Materials (IAM), Nanjing University of Posts &Telecommunications (NUPT), Nanjing 210023, P. R. China. E-mail: iamlhxie@njupt.edu.cn; iamwhuang@njupt.edu.cn

[b]Jiangsu-Singapore Joint Research Center for Organic/Bio Electronics & Information Displays, Institute of Advanced Materials (IAM), Nanjing University of Technology (NJUT), Nanjing 211816, P. R. China

[c]School of Electrical and Information, Northeast Agricultural University, Haerbin 150030, P. R. China

† Electronic supplementary information (ESI) available. See DOI: 10.1039/c3tc32460e

enhance the insulating capacity of the cross-linked PVP film using a simple fabrication process. In addition, the studies on the bending effect and mechanism on the electrical parameters of the flexible OTFTs, based on cross-linked PVP as the gate dielectric layer, during the mechanical bending process are rarely reported.

In this article, we fabricated high performance flexible OTFTs with a low operational voltage using two layers of cross-linked PVP as the dielectric layer and pentacene as the active layer on a flexible polyimide (PI) substrate. The variations on the electrical parameters of the flexible OTFTs as a function of the different bending radius and bending cycles were systematically characterized. Moreover, we further analyzed the causes which induced the variations in the electrical parameters of the flexible OTFTs during the mechanical bending process. Finally, we also investigated the electrical stability and the mechanical endurance of the flexible OTFTs under ambient conditions.

Experimental

Fig. 1(a) shows the schematic diagram of the flexible OTFTs which were fabricated with bottom-gate and top-contact structures. The 70 μm thick PI sheet was used as the substrate, and it was cleaned sequentially with acetone, ethanol, and deionized water, and then was dried; the residual solvent was removed by N_2 gas. Subsequently the PI substrate was baked at 120 °C for 20 mins in the oven to improve its flexibility and thermal stability. The gate electrode, about 150 nm thick aluminum (Al), was thermally evaporated on the PI substrate. The gate insulator layer, a cross-linked poly(4-vinylphenol) (PVP) solution, was prepared with 20 mg ml^{-1} PVP (Mw ~ 11 000) and 2 mg ml^{-1} 4-(hexafluoroisopropylidene)diphthalic anhydride (HDA) as the cross-linking agent, 1 μl ml^{-1} triethylamine (TEA) as the catalyst.[14] The solution was filtered through 0.22 μm membrane filters and was then continuously spin-coated onto the substrate at 2000 rpm for 45 s twice. Subsequently the substrate was transferred to the oven to be cross-linked for 2 hours at 100 °C in air. After that, the semiconductor layer, a 50 nm thick pentacene film, was thermally evaporated onto the gate insulator layer. Finally, the source (S) and drain (D), 50 nm thick gold (Au) electrodes, were deposited onto the pentacene film by thermal evaporation through a metal shadow mask. Fig. 1(b) shows a photograph of the flexible OTFT array fabricated on a PI substrate. The electrical characteristics of the flexible OTFTs were measured using an Agilent B1500A semiconductor parameter analyzer. All the measurements were carried out under ambient conditions where the humidity was controlled between 20% and 25% without any encapsulation.

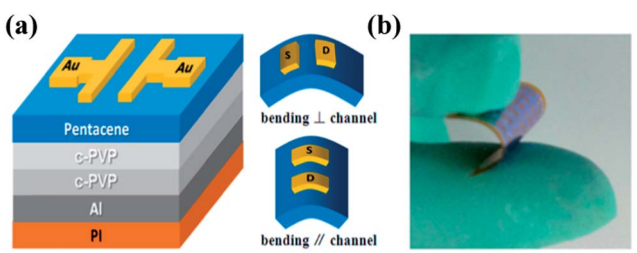

Fig. 1 (a) The schematic diagram of the flexible OTFTs. (b) A photograph of the flexible OTFT array fabricated on a PI substrate.

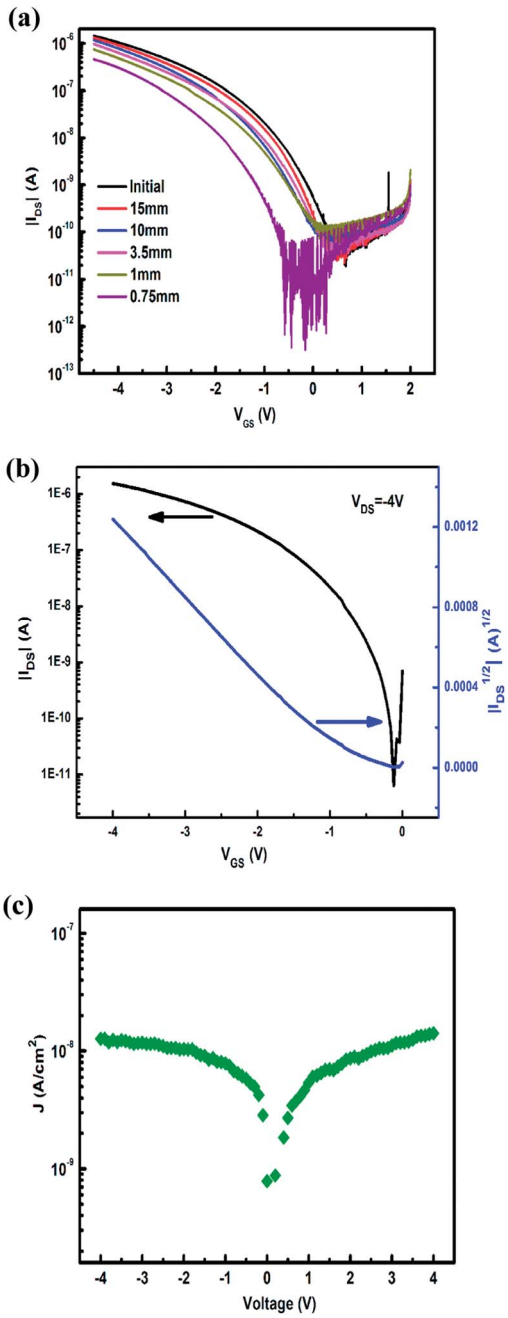

Fig. 2 The typical (a) output and (b) transfer characteristics of the flexible OTFTs with a channel width of 1500 μm and a length of 150 μm. (c) The electrical properties of the diodes with the structure of PI/Al/cross-linked PVP/PVP/pentacene/Au after 10^4 bending cycles at a bending radius of 3.5 mm.

Results and discussion

Fig. 2(a) shows the typical output characteristic of the flexible OTFTs. The source–drain current (I_{DS}) showed an obvious linear regime at lower source–drain voltages (V_{DS}) and a saturation regime at higher V_{DS}, indicating that an ohmic contact was well formed between the Au electrodes and pentacene films. Holes were also adequately accumulated in the conductive channel between the pentacene films and the cross-linked PVP layers. Fig. 2(b) shows the typical transfer characteristics of the flexible OTFTs with a channel width of 1500 μm and a length of 150 μm. The estimated saturation carrier mobility (μ), threshold voltage (V_{th}) and on/off current ratio of the flexible OTFTs were found to be 0.56 $cm^2\ V^{-1}\ s^{-1}$, −0.82 V and 10^5, respectively. The above parameters are comparable to those of rigid OTFTs.[15] Fig. 2(c) shows the electrical properties of the diodes with the structure of PI/Al/cross-linked PVP/PVP/pentacene/Au after 10^4 bending cycles at a bending radius of 3.5 mm. The current density (J) was only about 10^{-9} A cm^{-2} to 10^{-8} A cm^{-2} when the applied voltage swept between −4 V and +4 V. Moreover, as the applied voltage increased, the current density increased very slowly and tended to saturate. This shows that the electrical insulation of the cross-linked PVP film is good and can effectively prevent the carriers from the conductive channel diffusing into the insulator layer. It should be noted that the single layer cross-linked PVP film could be easily broken-down by applying an electric field due to the existence of pinholes. To solve this problem, we used two layers of cross-linked PVP film as the dielectric layer in the experiment, and the probability of these pinholes overlapping in each layer of the cross-linked PVP film is very small. Moreover, the flexible OTFTs still showed high performance at low operational voltages (≤−5 V). Therefore, the introduction of the two layers of cross-linked PVP film could enhance the insulating capacity of the gate dielectric layer and reduce the complexity of the fabrication technology by this simple fabrication process.

To explore the influence of the bending radius, the variations in electrical parameters of the flexible OTFTs with different bending radii were investigated. Fig. 3 shows the electrical characteristics of the flexible OTFTs as a function of the bending radius under a tensile bending mode with the channel direction oriented parallel to the bending direction. The variation of the transfer curves of the flexible OTFTs as a function of the bending radius is shown in Fig. 3(a). Although the transfer curves gradually shifted toward the negative direction with the decreasing bending radius, the flexible OTFTs still showed high performance characteristics. After 10^4 successive bending cycles, the field-effect mobility, threshold voltage and on/off current ratio of the flexible OTFTs at the bending radius of 1 mm were found to be 0.41 $cm^2\ V^{-1}\ s^{-1}$, −1.61 V and 10^4, respectively. This indicates that the flexible OTFTs have fine electrical properties and mechanical flexibilities. Fig. 3(b) shows the variation of the field-effect mobility and threshold voltage as a function of the bending radius. When the bending radius varied from 15 mm to 0.75 mm, the field-effect mobility decreased, and the absolute value of threshold voltage

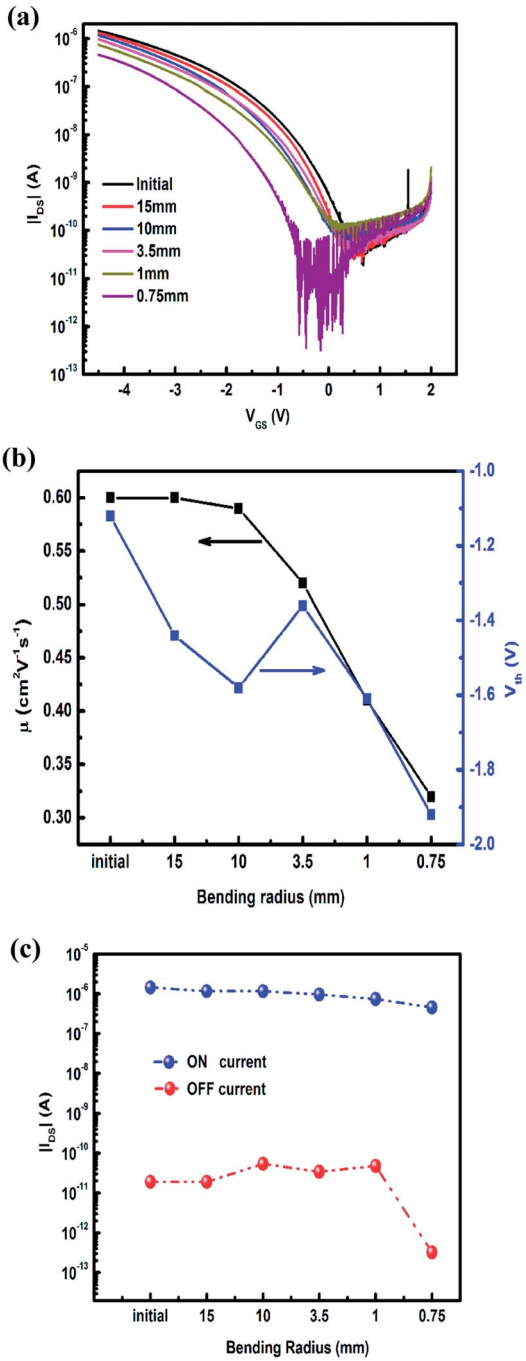

Fig. 3 The variation in the electrical characteristics of the flexible OTFTs as a function of the bending radius, including; (a) transfer curves, (b) field-effect mobility and threshold voltage and (c) on and off current.

increased. The degradation tendency of the field-effect mobility and threshold voltage are attributed to the larger spacing between pentacene molecules induced by the tensile strain.[16,17] It is well known that the charge transport in pentacene films is the hopping transport. The charge hopping transport rate is closely related to the field-effect mobility, and it is inversely proportional to the distance between hopping sites.[18,19] As the bending radius decreased, the distance between the

neighboring pentacene molecules increased under the tensile strain induced by the mechanical deformation. The charge hopping transport rate correspondingly decreased which caused the decrease in the field-effect mobility. Meanwhile, as the bending radius gradually became smaller, the number of charge traps in the conductive channel under the tensile strain increased which caused the increase in the threshold voltage.[20] Fig. 3(c) shows the variation in the on and off current of the flexible OTFTs as a function of the bending radius. The on current showed a slight reduction and the off current showed obvious fluctuation. The variation in the on and off current was mainly due to the following reasons; the off current is closely related to the electrical insulation of the dielectric layer, and the on current relies heavily on the conductivity of the organic semiconductor. When the flexible OTFTs were under different bending radii, the PVP layer would generate a certain degree of deformation induced by the mechanical bending and the electrical insulation of the cross-linked PVP also changed. However, the deformation degree of the PVP layer might be non-uniform which varied the insulating ability of the PVP layer, thus the off current showed corresponding fluctuation. The reduction of the on current was attributed to the conductivity degradation of the pentacene film caused by the mechanical bending.[16] However, compared to the change of the insulating ability of the PVP layer, the conductivity of pentacene film was relatively stable, so the change in the on current was smaller than that of the off current.

Fig. 4 shows the electrical characteristics of the flexible OTFTs as a function of the mechanical bending cycles with the bending direction aligned parallel and vertical to the channel direction. Compared to the initial transfer characteristics, most of the transfer curves of the flexible OTFTs with the bending direction aligned parallel as well as vertical to the channel direction, shifted toward the negative direction after successive mechanical bending. The negative shift of the transfer curves with the bending direction aligned vertical to the channel direction is more apparent, as shown in Fig. 4(a) and (b). It should be noted that the degree of negative shift of the transfer curves with the two bending directions did not increase with the increasing number of mechanical bending cycles. Even the individual transfer curve shifted toward the positive direction, as shown in Fig. 4(b), showing that the transfer curve shift of the flexible OTFTs was not proportional to the number of mechanical bending cycles. To explore the influence of the mechanical bending cycles, the variations in the electrical parameters of the flexible OTFTs with the mechanical bending cycles were investigated, as shown in Fig. 4(c)–(e). It can be seen that the variation in the field-effect mobility and the absolute value of the threshold voltage with the two bending directions became larger after 10^4 successive mechanical bending. Although the higher threshold voltage is unfavorable for flexible OTFTs, it was only within 2 V after the successive bending cycles which is still very low in the reported results of flexible OTFTs.[21,22] The variation trends of the field-effect mobility and threshold voltage are closely related to the increased hole concentration in the conductive channel. The pentacene films generated more cracks with the increase in the number of

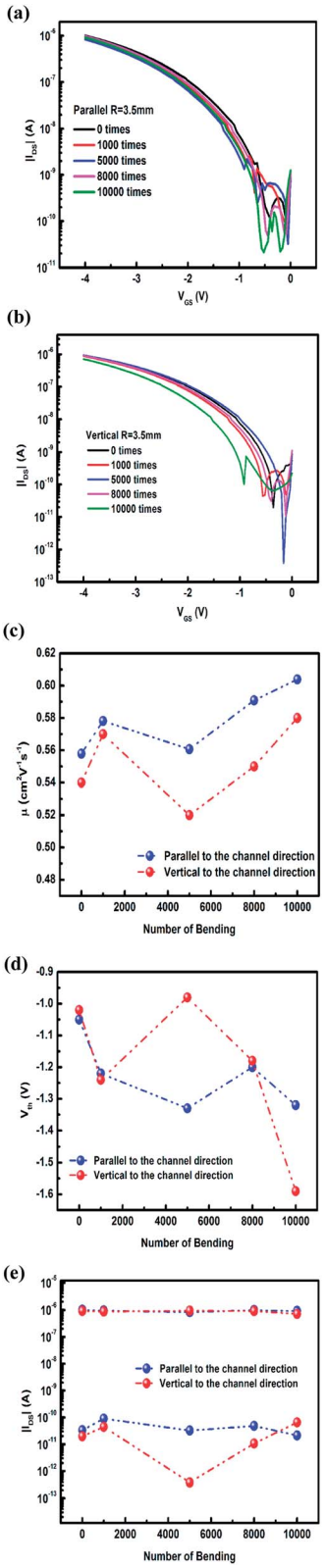

Fig. 4 The electrical characteristics of the flexible OTFTs as a function of the mechanical bending cycles with the bending direction aligned (a) parallel and (b) vertical to the channel direction. The variations in the electrical parameters of the flexible OTFTs with the mechanical bending cycles, including; (c) field-effect mobility, (d) threshold voltage and (e) on and off current.

mechanical bending cycles (see ESI Fig. S1(a) and (b)†).[23,24] Then more H_2O and O_2 molecules in the air could be absorbed by these cracks and could further react with pentacene near the conductive channel. This could produce a certain number of holes and carrier traps in the conductive channel, thus both the hole concentration and carrier traps increased in the conductive channel and caused the field-effect mobility and threshold voltage to increase after the successive bending cycles.[25,26] To verify the role of the H_2O and O_2 molecules in the air, we put the sample under a N_2 atmosphere which was produced by nitrogen gas from a N_2 cylinder and measured the electrical parameters of the flexible OTFTs. It was found that the variation scope of the field-effect mobility and the threshold voltage of the flexible OTFTs as a function of the mechanical bending cycles with a bending radius of 3.5 mm were smaller (see ESI Fig. S1(c) and (d)†). This indicates that the H_2O and O_2 molecules play the role of increasing the conductivity of the channel and the threshold voltage. The variation in the on and off current was different as the number of mechanical bending cycles increased, as shown in Fig. 4(e). During the successive mechanical bending cycles, the on current was nearly unchanged, but the off current showed obvious fluctuation. The variation tendency of the on and off current is consistent with the analysis in the previous paragraph. In addition, it can also be seen that the variation in the electrical parameters of the flexible OTFTs with the bending direction aligned vertically to the channel direction was more significant than the bending direction aligned parallel to the channel direction. These results showed the deformation induced by bending in the direction aligned vertically to the channel direction has greater influence on the carrier transport in the conductive channel of the flexible OTFTs.[27,28]

As mentioned above, the contrary change tendency of the flexible OTFTs as a function of bending radius and bending cycles was observed. The decrease of the field-effect mobility with the smaller bending radius was mainly due to the distance effect of spacing between the stretched pentacene molecules which was induced by the stronger strain. However, when the bending radius remained unchanged, the field-effect mobility of the flexible OTFTs increased with the increase in the number of bending cycles, the increased field-effect mobility was caused by the doping effect of H_2O and O_2 from the air. According to the variation of the field-effect mobility under the different mechanical bending tests, we deduced that the distance effect of the spacing between the stretched pentacene molecules and the doping effect of H_2O and O_2 should present simultaneously during the mechanical bending process. Fig. 5 shows the variation of the field-effect mobility as a function of the mechanical bending cycles with a larger bending radius (10 mm) and a smaller bending radius (3.5 mm). When the number of mechanical bending cycles was lower, the field-effect mobility of the flexible OTFTs for the two bending radii increased, indicating that the influence of the doping effect was dominant in this stage. As the number of mechanical bending cycles increased, the field-effect mobility of the two bending radii decreased, indicating that the influence of the distance effect played an important role in changing the field-effect mobility at this stage. In addition, the field-effect mobility of the flexible

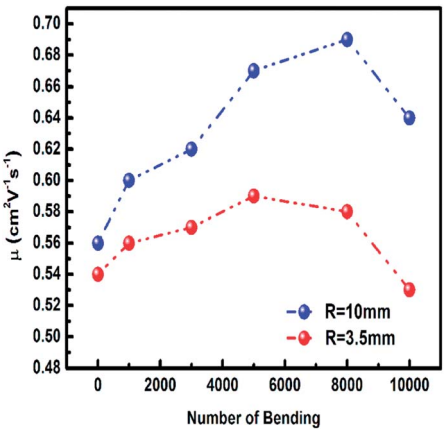

Fig. 5 The variation of the field-effect mobility as a function of the number of mechanical bending cycles with a large bending radius (10 mm) and a small bending radius (3.5 mm).

OTFTs with a bending radius of 3.5 mm decreased less than when the bending radius of 10 mm, indicating that distance effect has a stronger influence on the field-effect mobility with a smaller bending radius. These results further verified our deduction that the distance effect and doping effect are mutually independent as well as mutually related during the mechanical bending process. That is, when the mechanical deformation degree of the flexible OTFTs was smaller, the distance between the neighboring pentacene molecules only slightly changed due to the intermolecular forces of the pentacene molecules, thus the distance effect caused by the mechanical deformation had little influence on the field-effect mobility of the flexible OTFTs. H_2O and O_2 molecules in the air could be easily absorbed by the cracks caused by the mechanical deformation in the pentacene layer and could enhance the hole concentration in the conductive channel. In this case, the doping effect rather than distance effect had a greater influence on the field-effect mobility of the flexible OTFTs. When the mechanical deformation degree of the flexible OTFTs was larger, the changes in the distance between the neighboring pentacene molecules obviously increased which caused the charge hopping transport rate to decrease. Although the influence of the doping effect caused by H_2O and O_2 molecules still existed, the influence of the distance effect caused by the spacing between the stretched pentacene molecules was dominant in changing the field-effect mobility of the flexible OTFTs. Our research results are different compared with the previous studies which reported there was only one mechanism for the change in the field-effect mobility during the mechanical bending process of the OTFTs.[23,29] Therefore, our studies are very helpful to further understand the relationship between the bending method and the performance of the OTFTs.

Fig. 6(a) shows the electrical characteristics of the flexible OTFTs under the bending states. The relatively small shift of the transfer curves can be observed even if the bending time is approximately 2 hours at a radius of 1 mm. When the flexible OTFTs were held under the bending state, the field-effect

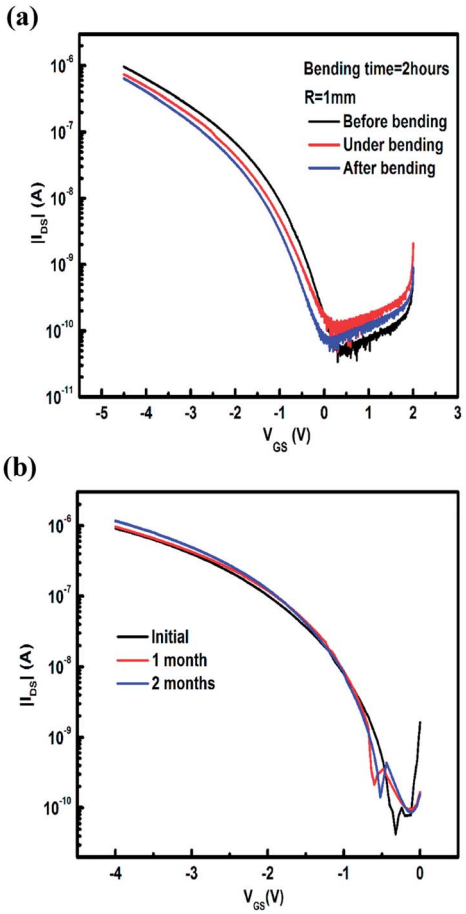

Fig. 6 (a) The electrical characteristics of the flexible OTFTs (a) under the bending state and (b) without a passivation layer in ambient conditions for 2 months.

mobility, threshold voltage and on/off current ratio at a bending radius of 1 mm still remained at 0.52 $cm^2 V^{-1} s^{-1}$, −1.61 V and 10^4, respectively. These results show that the flexible OTFTs exhibited high mechanical flexibility and electrical performance. Fig. 6(b) shows the electrical characteristics of the flexible OTFTs without a passivation layer under ambient conditions for 2 months. It can be seen that there was no noticeable degradation of the performance of the flexible OTFTs during these 2 months, indicating that our devices have excellent electrical stabilities under ambient conditions. Moreover, the flexible OTFTs still operated well after 2 months, and the field-effect mobility, threshold voltage and on/off current ratio of the flexible OTFTs were 0.53 $cm^2 V^{-1} s^{-1}$, −1.07 V and 10^4, respectively.

Conclusions

In conclusion, we have demonstrated high performance flexible OTFTs using cross-linked PVP as the dielectric layers on a PI substrate. After a series of severe mechanical bending tests, the flexible OTFTs still showed excellent mechanical flexibility, electrical performance and electrical stability at the lower operational voltages under ambient conditions. From the results of the variations of the electrical parameters of the flexible OTFTs during the mechanical bending process, we found that the opposite variation of the field-effect mobility as a function of the bending radius and number of bending cycles was due to the distance effect of spacing between the stretched pentacene molecules and the doping effect of H_2O and O_2 which were induced by the mechanical bending strain. Moreover, further research results showed that the distance effect and the doping effect are mutually independent as well as mutually related during the mechanical bending process. Our results provide valuable information to help understand the mechanical bending effect of flexible OTFTs.

Acknowledgements

The project was supported by the National Basic Research Program of China (2012CB723402, 2014CB648300), the National Natural Science Foundation of China (61204095, 61136003, 21144004, 61377019, 61106116), the National Science Fund for Excellent Young Scholars (21322402), the Key Project of Chinese Ministry of Education, China (20113223120003), the Natural Science Foundation of Jiangsu Province, China (BK2012431), the Natural Science Foundation of the Education Committee of Jiangsu Province, China (11KJB510017), and the Scientific Research Staring Foundation of Nanjing University of Posts and Telecommunications, China (NY211022).

Notes and references

1 T. Sekitani, U. Zschieschang, H. Klauk and T. Someya, *Nat. Mater.*, 2010, **9**, 1015.
2 H. T. Yi, M. M. Payne, J. E. Anthony and V. Podzorov, *Nat. Commun.*, 2012, **3**, 1259.
3 J. Dong, Y.-H. Chai, Y.-Z. Zhao, W.-W. Shi, Y.-X. Guo, M.-D. Yi, L.-H. Xie and W. Huang, *Chin. Phys. B*, 2013, **62**, 047301.
4 G. H. Gelinck, H. E. A. Huitema, E. Van Veenendaal, E. Cantatore, L. Schrijnemakers, J. Van der Putten, T. C. T. Geuns, M. Beenhakkers, J. B. Giesbers, B. H. Huisman, E. J. Meijer, E. M. Benito, F. J. Touwslager, A. W. Marsman, B. J. E. Van Rens and D. M. De Leeuw, *Nat. Mater.*, 2004, **3**, 106.
5 Q. Cao, S. H. Hur, Z. T. Zhu, Y. G. Sun, C. J. Wang, M. A. Meitl, M. Shim and J. A. Rogers, *Adv. Mater.*, 2006, **18**, 304.
6 H. Sirringhaus, *Proc. IEEE*, 2009, **97**, 1570.
7 K.-J. Baeg, D. Khim, J. Kim, B.-D. Yang, M. Kang, S.-W. Jung, I.-K. You, D.-Y. Kim and Y.-Y. Noh, *Adv. Funct. Mater.*, 2012, **22**, 2915.
8 K.-J. Baeg, Y.-Y. Noh, H. Sirringhaus and D.-Y. Kim, *Adv. Funct. Mater.*, 2010, **20**, 224.
9 S. K. Hwang, I. Bae, R. H. Kim and C. Park, *Adv. Mater.*, 2012, **24**, 5910.
10 D. Ji, L. Jiang, X. Cai, H. Dong, Q. Meng, G. Tian, D. Wu, J. Li and W. Hu, *Org. Electron.*, 2013, **14**, 2528.

11 T. Sekitani, T. Yokota, U. Zschieschang, H. Klauk, S. Bauer, K. Takeuchi, M. Takamiya, T. Sakurai and T. Someya, *Science*, 2009, **326**, 1516.

12 M. Kaltenbrunner, P. Stadler, R. Schwödiauer, A. W. Hassel, N. S. Sariciftci and S. Bauer, *Adv. Mater.*, 2011, **23**, 4892.

13 Y. Chung, E. Verploegen, A. Vailionis, Y. Sun, Y. Nishi, B. Murmann and Z. Bao, *Nano Lett.*, 2011, **11**, 1161.

14 M. E. Roberts, N. Queralto, S. C. B. Mannsfeld, B. N. Reinecke, W. Knoll and Z. Bao, *Chem. Mater.*, 2009, **21**, 2292.

15 M. Uno, Y. Hirose, T. Uemura, K. Takimiya, Y. Nakazawa and J. Takeya, *Appl. Phys. Lett.*, 2010, **97**, 013301.

16 V. Scenev, P. Cosseddu, A. Bonfiglio, I. Salzmann, N. Severin, M. Oehzelt, N. Koch and J. P. Rabe, *Org. Electron.*, 2013, **14**, 1323.

17 Y. Zhou, S.-T. Han, Z.-X. Xu and V. A. L. Roy, *Nanoscale*, 2013, **5**, 1972.

18 R. P. Ortiz, A. Facchetti and T. J. Marks, *Chem. Rev.*, 2010, **110**, 205.

19 A. Nigam, G. Schwabegger, M. Ullah, R. Ahmed, I. I. Fishchuk, A. Kadashchuk, C. Simbrunner, H. Sitter, M. Premaratne and V. R. Rao, *Appl. Phys. Lett.*, 2012, **101**, 083305.

20 P. Heremans, G. H. Gelinck, R. Muller, K.-J. Baeg, D.-Y. Kim and Y.-Y. Noh, *Chem. Mater.*, 2011, **23**, 341.

21 H. Y. Noh, Y. G. Seol and N. E. Lee, *Appl. Phys. Lett.*, 2009, **95**, 113302.

22 Y. G. Seol, H. Y. Noh, S. S. Lee, J. H. Ahn and N. E. Lee, *Appl. Phys. Lett.*, 2008, **93**, 013305.

23 Y. G. Seol, N. E. Lee, S. H. Park and J. Y. Bae, *Org. Electron.*, 2008, **9**, 413.

24 Y. G. Seol, J. G. Lee and N. E. Lee, *Org. Electron.*, 2007, **8**, 513.

25 Y. Zhou, S.-T. Han, Z.-X. Xu and V. A. L. Roy, *Nanotechnology*, 2012, **23**, 344014.

26 S.-T. Han, Y. Zhou, C. Wang, L. He, W. Zhang and V. A. L. Roy, *Adv. Mater.*, 2013, **25**, 872.

27 R. Nakahara, M. Uno, T. Uemura, K. Takimiya and J. Takeya, *Adv. Mater.*, 2012, **24**, 5212.

28 H. Gleskova, S. Wagner, W. Soboyejo and Z. Suo, *J. Appl. Phys.*, 2002, **92**, 6224.

29 J.-M. Kim, T. Nam, S. J. Lim, Y. G. Seol, N. E. Lee, D. Kim and H. Kim, *Appl. Phys. Lett.*, 2011, **98**, 142113.